Dissociation of diatomic molecules and the exact-exchange Kohn-Sham potential: The case of LiF

Adi Makmal,[1] Stephan Kümmel,[2] and Leeor Kronik[1]
[1]*Department of Materials and Interfaces, Weizmann Institute of Science, Rehovoth 76100, Israel*
[2]*Physikalisches Institut, Universität Bayreuth, D-95440 Bayreuth, Germany*
(Received 6 March 2011; published 21 June 2011)

We examine the role of the exact-exchange (EXX) Kohn-Sham potential in curing the problem of fractional molecular dissociation. This is achieved by performing EXX calculations for the illustrative case of the LiF molecule. We show that by choosing the lowest-energy electronic configuration for each interatomic distance, a qualitatively correct binding energy curve, reflecting integer dissociation, is obtained. Surprisingly, for LiF this comes at the cost of violating the Aufbau principle, a phenomenon we discuss at length. Furthermore, we numerically confirm that in the EXX potential of the diatomic molecule, one of the atomic potentials is shifted by a constant while the other one is not, depending on where the highest occupied molecular orbital is localized. This changes the relative positions of the energies of each atom and enforces the integer configuration by preventing spurious charge transfer. The size of the constant shift becomes increasingly unstable numerically the larger the interatomic separation is, reflecting the increasing absence of coupling between the atoms.

DOI: 10.1103/PhysRevA.83.062512 PACS number(s): 31.15.E−

I. INTRODUCTION

The improper dissociation of neutral "highly stretched" diatomic molecules into fractionally charged fragments $X^{+q} \cdots Y^{-q}$ is a well-known problem within density-functional theory (DFT) [1–22]. For example, the local density approximation (LDA) yields $q = 0.25$ for LiH [1], $q = 0.4$ for NaCl [3,10] and LiF [7], and $q = 0.2$ for FH [21]. This problem is pervasive. Ruzsinszky *et al.* have shown that LDA erroneously predicts fractional dissociation for 174 of the 276 distinct heteroatomic dimers one can form from the first 24 open *sp*-shell atoms [10]. Furthermore, fractional dissociation is often found even when using more sophisticated families of functionals, including the generalized gradient approximation (GGA) [8,10,12,13], meta-GGA [10], or hybrid functionals employing a fixed fraction of exact exchange (EXX) [8,12,13].

For semilocal functionals, this serious deficiency is attributed to the inherent problems of the presence of a self-interaction error [10,13] and the absence of a derivative discontinuity in the exchange-correlation potential [1]—issues that are not unrelated [4,23]. Correspondingly, neutral charge dissociation has been achieved with the Perdew-Zunger [24] self-interaction correction (SIC) scheme [10,13], Hartree-Fock (HF) theory [8,10], and the range-split hybrid [21,23] (RSH) functional approach [12,13,21]. All of these methods are rigorously (SIC, HF) or at least asymptotically (RSH) self-interaction-free (self-interaction is mitigated, but not eliminated, in hybrid functionals), see, e.g., [23]. But they circumvent, to varying degrees and in different ways, the derivative discontinuity issue by employing nonlocal potential operators.

Use of a nonlocal potential operator, however, should not be an essential ingredient to overcoming the fractional dissociation problem. On general grounds, the Kohn-Sham (KS) theory [25], which employs a local potential, is in principle exact and should correctly predict any ground-state property, including molecular dissociation. For example, a KS SIC scheme involving localizing transformations has been shown to yield the correct dissociation curve of He_2^+ [26]. Furthermore, detailed analysis of the exact functional reveals the special structure of the exact exchange-correlation potential that makes this possible in practice [4,5,17,18], an issue elaborated below.

EXX employed within KS theory, i.e., with a local potential obtained from the optimized effective potential (OEP) equation [23,27–31] (or approximations thereof), exhibits a derivative discontinuity and is also self-interaction free. Just like HF theory, it does not account for correlation. However, it differs from HF theory due to the different potential operators. Therefore, EXX and HF theory each possess components that the other would "view" as correlation [6,23]. It is thus interesting to examine whether EXX is generally sufficient for overcoming the fractional dissociation problem [32] and, if so, what is the nature of the local KS potential that allows for this. Here, we answer this question by performing EXX calculations on the illustrative case of the LiF molecule. We show that by choosing the lowest-energy electronic configuration for each interatomic distance, we can obtain a binding energy curve that is qualitatively correct and has the same structure of the HF ones. We further demonstrate the mechanism through which a local potential can lead to neutral dissociation and present a detailed analysis of its "step structure" features. The study gains further significance as the physics of this "step structure" in the exchange-correlation potential, which is at the heart of the dissociation problem, is also highly relevant to problems of ionization by external fields [33,34].

II. COMPUTATIONAL DETAILS

All EXX calculations were performed using DARSEC [35]—a recently developed all-electron code for diatomic molecules, based on a real-space prolate-spheroidal-coordinate grid. Here, this is useful because the nonuniform grid is inherently denser near the nuclei and sparser far from them, facilitating an accurate numerical solution even for large bond lengths. The local exchange potential was found using the Krieger, Li, and Iafrate (KLI) approximation [36] to the OEP equation. All calculations were spin-unrestricted and total energies were converged to at least 0.01 Ry.

It was often our experience, especially for large interatomic separations, that an electronic configuration which violates the Aufbau principle was more energetically stable than the one obeying it. We elaborate on this point in Sec. III 4. To converge an electronic configuration tending toward neutral or ionic fragments irrespective of the Aufbau principle we followed a two-step procedure: First, the atomic charge q in $Li^{+q}\cdots F^{-q}$ was estimated for any bond length, R, by a real-space integration of the density "belonging" to each atom (followed by adding the nuclear charge). This scheme for calculating q is by no means a uniquely defined one [37–39]. Here we simply integrated the density in the half-space closer to each atom, using the fact that division into two half-spaces is inherent in the prolate-spheroidal coordinate grid (see Fig. 1 in Ref. [35]). For large R, this naive scheme is sufficient to produce a value that approaches our intuitive notion of atomic charges. Then, in the second and final step, if an ionic (neutral) configuration was desired, and q was found to be smaller (larger) than some threshold value (0.35 in the present work), the electron residing on the highest occupied orbital belonging to the cation (anion) was transferred to the lowest unoccupied orbital of the anion (cation) within the same spin channel. These two steps were taken after each cycle in the self-consistency procedure to prevent the system from reverting to the Aufbau-obeying configuration.

III. RESULTS AND DISCUSSION

1. Binding energy and charge curves

Binding energy curves of LiF (the reference total energies for Li and F are given in Table I below), computed for both the "ionic" and "neutral" configurations, are shown in Fig. 1(a). The neutral configuration does not obey the Aufbau principle, and was obtained as discussed above. Nevertheless, Fig. 1(a) shows that for large R it is clearly the more energetically stable one. For each configuration, curves of the fractional charge on the Li atom are shown in Fig. 1(b). Next, by choosing the energetically stable configuration for each R, we obtain the overall binding energy and fractional charge curves, as shown in Figs. 1(c) and 1(d), respectively. It is immediately obvious that fractional dissociation does not arise and that for $R\to\infty$, $q\to 1$ in the ionic configurations and $q\to 0$ in the neutral one.

Figure 1(c) demonstrates that despite the use of a local potential, EXX calculations that are done within the KLI approximation (xKLI) are sufficient to obtain a qualitatively correct binding energy curve which restores neutral dissociation. Furthermore, Fig. 1(d) shows that the fractional charge increases toward 1 until a critical distance of $6.5 < R_c < 7.0$ a.u., following which it abruptly drops to near 0. This agrees well with an independent estimate of the critical distance, based on the relation [1]

$$R_c = e^2/(I_{\rm Li} - A_{\rm F}), \tag{1}$$

where $e^2 = 2$ because Rydberg atomic units are used throughout, $I_{\rm Li}$ is the ionization potential of Li, and $A_{\rm F}$ is the electron affinity of F. If both $I_{\rm Li}$ and $A_{\rm F}$ are computed within xKLI from total energy differences, a critical value of 6.7 a.u. is obtained [using the experimental values in Eq. (1) was shown in Ref. [13] to yield a much larger estimation of $R_c \simeq$ 13.6 a.u.]. We further note that this behavior, which is similar to the one famously discussed by Coulson and Fischer [40], is qualitatively the same as that obtained from HF theory for LiF (with a similar critical distance of $R_c \simeq 6.6$ a.u.) [13] and for NaCl [10], again demonstrating that a nonlocal potential is not essential.

2. Potential structure

To explain how exact KS theory can describe charge dissociation correctly, Perdew has suggested in 1990 the following mechanism, taking NaCl as a representative case [4]: *"The exact KS potential maintains this situation [atomic neutrality—the authors] by erecting a 'plateau' of positive constant potential in the 'domain' of the Cl atom (that region of space in which the density of the Cl dominates that of the Na atom)."* To examine how this mechanism is reflected in our calculations, we consider the xKLI potential along the interatomic axis (shown as a solid line in Fig. 2) for both the ionic and the neutral configurations, in a highly stretched geometry with $R = 18$ a.u.

For the stretched ionic configuration, $Li^{+1}\cdots F^{-1}$ (top of Fig. 2), no spin polarization was found. For the neutral configuration, $Li^0\cdots F^0$ (bottom of Fig. 2), although each spin channel contains the same number of electrons, the spin symmetry is broken (as discussed recently in Ref. [22]) and

TABLE I. Ground-state xKLI energy levels (the last state is the lowest unoccupied one) and total energies (in Ry) of Li, F, and $Li^0\cdots F^0$ ($R = 18$ a.u.). The values of $\Delta_{H-1,\alpha}$ and $\Delta_{H-4,\beta}$ are also reported for the stretched molecule.

Li		F		$Li^0\cdots F^0$	
$\varepsilon_{i\alpha}$	$\varepsilon_{i\beta}$	$\varepsilon_{i\alpha}$	$\varepsilon_{i\beta}$	$\varepsilon_{i\alpha}$	$\varepsilon_{i\beta}$
−4.163	−4.934	−49.29	−49.40	−49.16(F)	−49.29(F)
−0.392	–	−2.93	−2.75	−4.163(Li)	−4.78(Li)
−0.257	−0.605	−1.56	−1.40	−2.50(F)	−2.93(F)
$E_{\rm tot} = -14.8648$		−1.56	−1.34	−1.16(F)	−1.56(F)
		−1.46	–	−1.09(F)	−1.56(F)
		−0.58	−1.34	−0.392(Li)	−1.46(F)
		$E_{\rm tot} = -198.8198$		−1.09(F)	−0.454(Li)
				$\Delta_{H-1} = 0.246$	$\Delta_{H-4} = 0.15$
				$E_{\rm tot} = -213.69$	

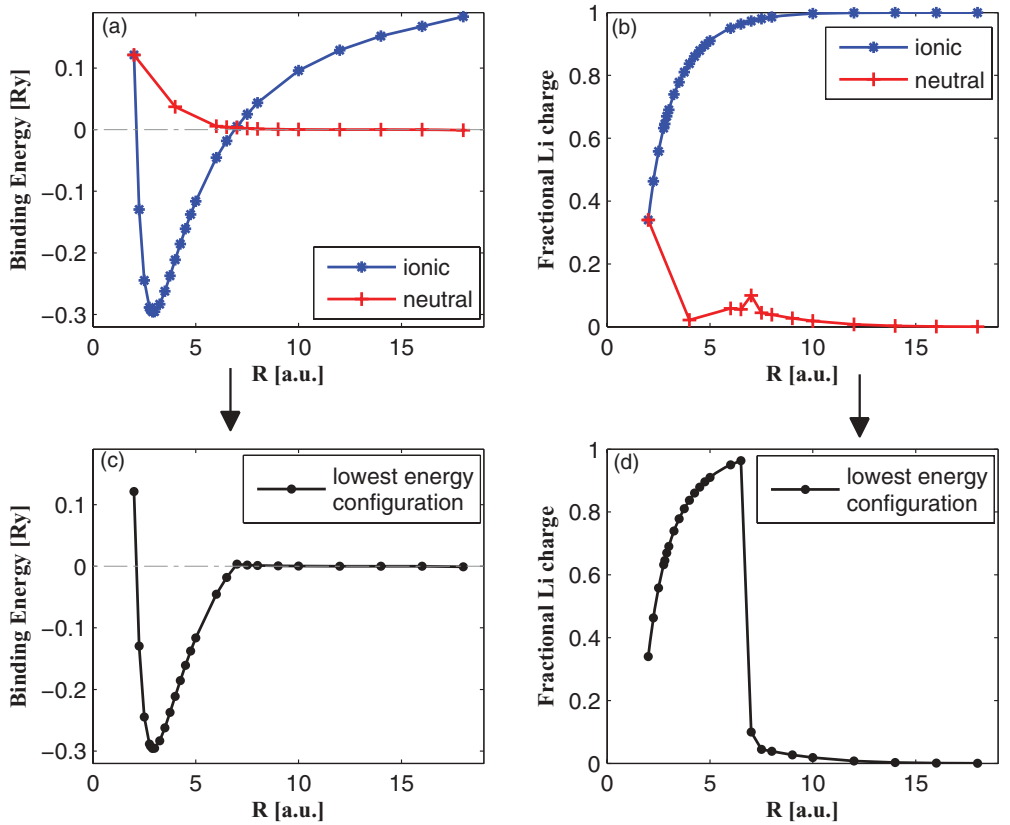

FIG. 1. (Color online) The LiF diatomic molecule. Left column: binding energy curves (in Ry) as a function of the interatomic distance R (in a.u.). Right column: fractional charge on the Li atom as a function of R (in a.u.). First row: both ionic and neutral configurations are plotted in blue stars and red plus signs, respectively. Second row: only the lowest energy configuration is plotted for each interatomic distance.

significant spin polarization is found. The potential shown corresponds to the α-spin channel, containing the majority-spin electrons of the Li atom (the potential corresponding to the β spin is qualitatively the same as that of the ionic one and is therefore not shown).

For the ionic configuration, the asymptotic potential in the "domain" of the F atom is a simple Coulomb potential ($-2/r$, in Ry units, shown as a dash-dotted line). In the "domain" of the Li atom, however, the potential tends toward a *different* asymptotic limit, shifted from $-2/r$ by a constant (see dashed line). For the neutral configuration, the picture is similar, except that it is the asymptotic potential in the Li "domain" that decays to zero and the asymptotic potential on the F "domain" that tends toward a positive constant. In other words, the Li and F asymptotic potentials are shifted with respect to each other by a constant. To bridge across this constant, a step in the potential must arise in between the atoms. This step is pointed out in Fig. 2 as s_1. It can be interpreted as enforcing nonfractional occupation by setting up a potential barrier that aims to prevent electron transfer from F to Li or from Li to F, for the ionic and neutral configurations, respectively. Accordingly, s_1 is of opposite sign in the two cases. Furthermore, the asymptotic positive-constant region of the shifted potential (dashed line) can be identified with Perdew's plateau. Because a finite object can have only one asymptotic KS potential [41,42], far to the left of the Li "domain" for the ionic configuration, or far to the right of the F "domain" in the neutral configuration, the above-mentioned positive asymptotic constant vanishes and the potential can no longer follow Perdew's plateau. This necessitates a second step in the potential profile, which is pointed out in Fig. 2 as s_2. This second step enforces the correct asymptotic structure of the potential with no further consequence for charge transfer.

The unique structure of the KS potential—a plateau accompanied by two potential steps of different signs—can be explained by examining the KLI approximation in more detail. The KLI potential (in the noncomplex formalism used in this work) is given by [29,43]

$$V_{\mathrm{xc},\sigma}^{\mathrm{KLI}}(\mathbf{r}) = \frac{1}{\rho_\sigma(\mathbf{r})} \sum_{i=1}^{N_\sigma} |\phi_{i\sigma}(\mathbf{r})|^2 \left[u_{i\sigma}(\mathbf{r}) + \overline{V}_{\mathrm{xc},i\sigma}^{\mathrm{KLI}} - \overline{u}_{i\sigma} \right], \qquad (2)$$

where σ is a spin index, $\phi_{i\sigma}(\mathbf{r})$ is the ith KS orbital, $u_{i\sigma}(\mathbf{r}) = \frac{1}{\phi_{i\sigma}^*(\mathbf{r})} \frac{\delta E_{\mathrm{xc}}}{\delta \phi_{i\sigma}(\mathbf{r})}$ with E_{xc} being the employed exchange-correlation energy functional, $\overline{V}_{\mathrm{xc},i\sigma}^{\mathrm{KLI}} = \langle \phi_{i\sigma} | V_{\mathrm{xc},\sigma}^{\mathrm{KLI}} | \phi_{i\sigma} \rangle$, and similarly $\overline{u}_{i\sigma} = \langle \phi_{i\sigma} | u_{i\sigma} | \phi_{i\sigma} \rangle$. In regions where the density is dominated by a single KS orbital, i.e., $\rho_\sigma(\mathbf{r}) \simeq |\phi_{k\sigma}(\mathbf{r})|^2$, the KLI potential reduces to (see, e.g., [44])

$$V_{\mathrm{xc},\sigma}^{\mathrm{KLI}}(\mathbf{r}) \simeq u_{k\sigma}(\mathbf{r}) + \Delta_{k\sigma}, \qquad (3)$$

where $\Delta_{k\sigma}$ stands for $\bar{V}_{\mathrm{xc},k\sigma}^{\mathrm{KLI}} - \bar{u}_{k\sigma}$.

In the case of EXX, $u_{i\sigma}(\mathbf{r})$ corresponding to the asymptotically dominating orbital tends to $-2/r$ for large r [45]. By extension, any asymptotic region that is dominated by a single orbital, $\phi_{k\sigma}(\mathbf{r})$, would feature an xKLI potential that

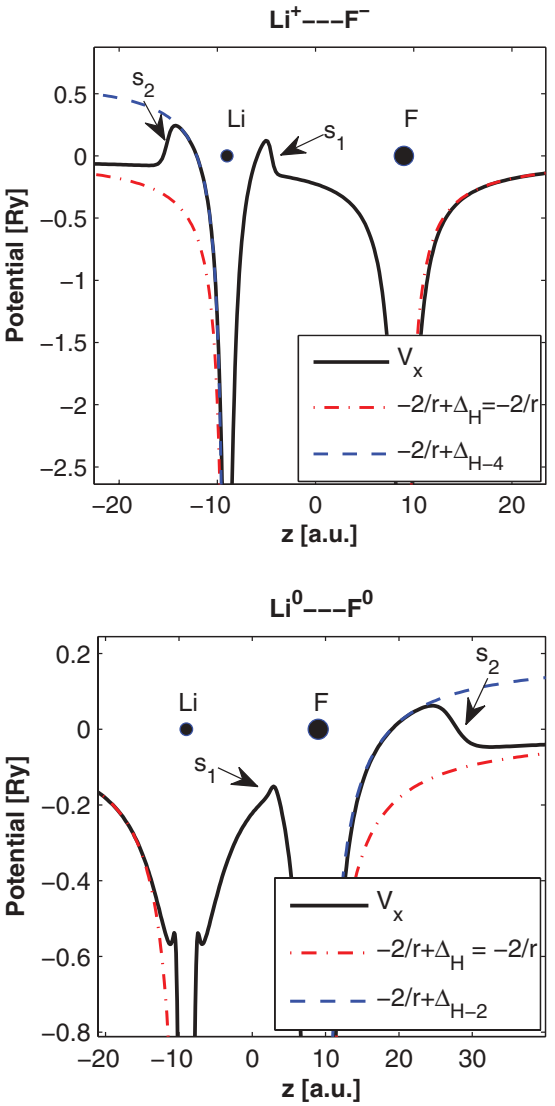

FIG. 2. (Color online) xKLI potential (black solid line) along the interatomic axis of the stretched LiF molecule with $R = 18$ a.u. Rydberg atomic units, i.e., $e^2 = 2$, are used. The potential tends to $-2/r$ (dash-dotted red line) far on either the Li or the F side. Top: $Li^{+1}\cdots F^{-1}$, the potential tends to $-2/r + \Delta_{H-4}$ (dashed blue line) near the Li atom. The $H-k$ subscript denotes the orbital that is k states below the HOMO. Bottom: $Li^0\cdots F^0$, the α-spin potential tends to $-2/r + \Delta_{H-2}$ (dashed blue line) near the F atom.

approaches $-2/r + \Delta_{k\sigma}$. Because each KS orbital is known to decay exponentially, with the decay constant dictated by the KS eigenvalue [29], at the asymptotic regime far to either the left or the right of the stretched molecule, the density must be dominated by the highest occupied molecular orbital (HOMO). Typically, the constant corresponding to this HOMO, Δ_H, is explicitly set to zero, yielding the correct asymptotic limit of $-2/r$ [36,44,46] that is indeed revealed in Fig. 2.

For a sufficiently stretched molecule where fractional dissociation is avoided, each orbital will be localized on one of the atoms. Consequently, the "domain" of each atom will be dominated by the HOMO of that atom, which is not necessarily the HOMO of the whole system (say, k eigenvalues lower). In such a "domain," the potential will approach a different

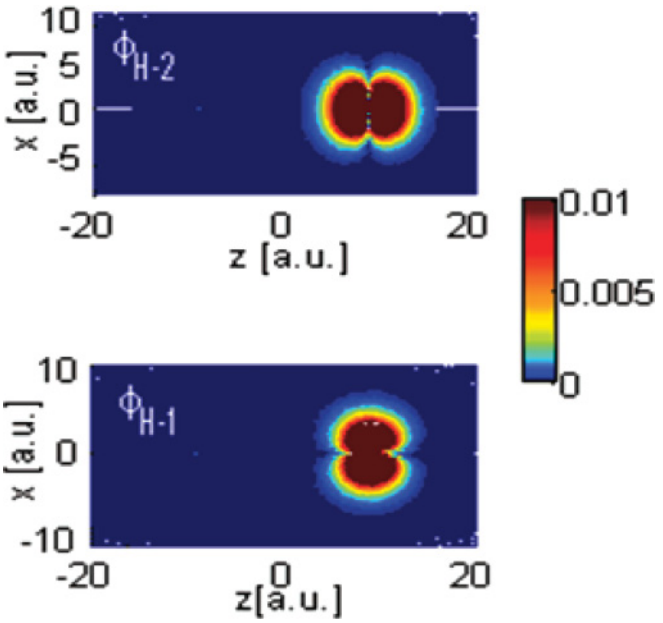

FIG. 3. (Color online) Two-dimensional view of the spin-α HOMO-2 and HOMO-1 orbitals of $Li^0\cdots F^0$ (Li on the left and F atom on the right) with $R = 18$ a.u., calculated with xKLI. Both orbitals are localized on the F atom, with p_z and p_x shapes, respectively, without and with a node along the interatomic axis.

asymptotic limit, $-2/r + \Delta_{H-k}$. Perdew's plateau is then an automatic consequence of Δ_{H-k} being nonzero. Specifically, for $Li^{+1}\cdots F^{-1}$, the HOMO of either spin channel resides on the F atom and HOMO-4 is the highest occupied orbital that is localized on the Li atom. Consequently, the F-related potential is not shifted ($\Delta_H = 0$) but the Li-related potential is shifted upward by Δ_{H-4}. Conversely, for $Li^0\cdots F^0$ in the α-spin channel, the HOMO resides on the Li atom and therefore it is the F-related potential that is shifted upward. The same argument also allows for the formation of the steps s_1 and s_2. These naturally arise in the area corresponding to the transition from a density dominated by the leading orbital of one atom to a density dominated by the leading orbital of the other atom.

We observe that for $Li^0\cdots F^0$ (bottom of Fig. 2), the shift of the potential on the F "domain" is dictated by Δ_{H-2}, even though the highest occupied orbital in the domain of the F atom is actually the HOMO-1. This seeming contradiction to the above argument arises because for the HOMO-1 orbital the interatomic axis is a nodal one, as shown in Fig. 3, whereas the HOMO-2 orbital does not possess a node along this axis and therefore dominates the density along it, leading to a "ridge" in the potential landscape. A similar behavior was previously reported and similarly explained in the context of EXX calculations of ethylene and benzene [44,47] and of Na_4 [48].

We note in passing that the phenomenon of shifts in the local EXX potential has been previously noted also for lower-lying orbitals of atoms [46,49,50] and is also observed here in our xKLI calculations. For example, Fig. 4 shows that in the domain of both Li and F there is a transition in the core region from domination by a $1s$ electron (HOMO-4 for Li, HOMO-5 for F) to domination by a valence electron (HOMO for Li, HOMO-2 for F). The transition of the potential from

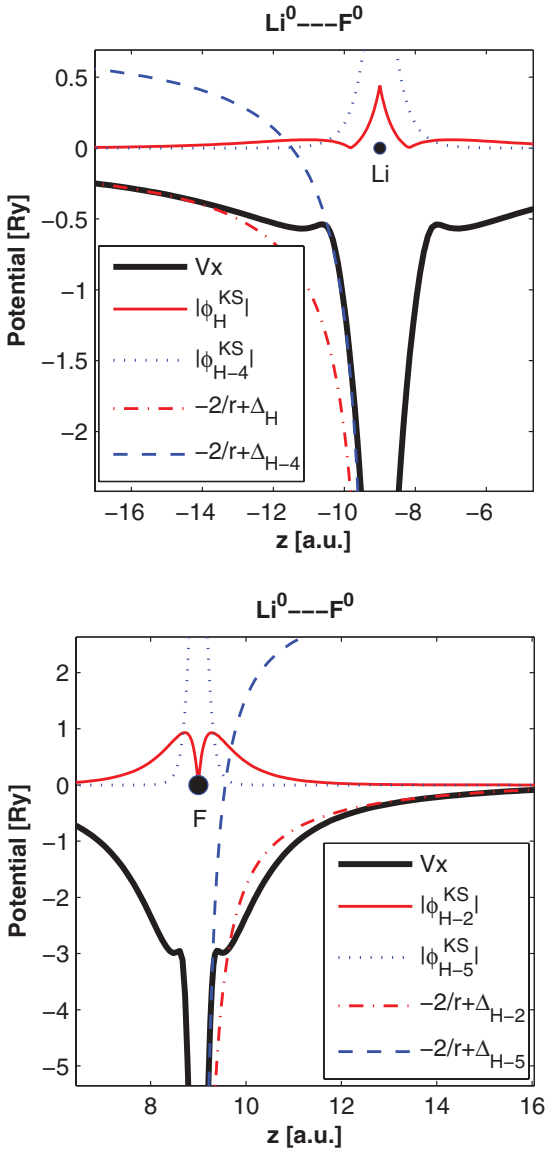

FIG. 4. (Color online) α-spin xKLI potential (in Ry, thick solid black line) and absolute value of KS orbitals (in arbitrary units), for $Li^0 \cdots F^0$ with $R = 18$ a.u., shown along the interatomic axis. Top: Focus on the Li atom, the HOMO $|\phi_H|$ and the $1s$ orbital $|\phi_{H-4}|$ are plotted in thin solid red line and dotted blue line, respectively. The potential tends to either $-2/r + \Delta_H = -2/r$ (dash-dotted red line) or $-2/r + \Delta_{H-4}$ (dashed blue line), depending on which orbital dominates. Bottom: Focus on the F atom, $|\phi_{H-2}|$ and the $1s$ orbital $|\phi_{H-5}|$ are shown in thin solid red line and dotted blue line, respectively. The potential tends to either $-2/r + \Delta_{H-2}$ (dash-dotted red line) or $-2/r + \Delta_{H-5}$ (dashed blue line), depending on which orbital dominates.

$-2/r+\Delta_{H-4}$ to $-2/r+\Delta_H$ for Li and from $-2/r+\Delta_{H-5}$ to $-2/r+\Delta_{H-2}$ for F occurs at the crossover point of orbital domination and is accompanied by a "bump" in the potential.

3. *Atom decoupling*

A subtle point involving the plateau and steps structure discussed above is its limiting behavior with an arbitrarily large interatomic distance. We remind the reader that in the KLI approach, all constant terms $\Delta_{i\sigma}$ are determined, for each spin σ, by solving a set of linear equations of the form $(I - M_\sigma)\Delta_\sigma = \bar{V}^S_\sigma - \bar{u}_\sigma$, where I is the identity matrix, Δ_σ is a vector of $\Delta_{i\sigma}$ values, $\bar{V}^S_\sigma$ is a vector consisting of $\bar{V}^S_{i\sigma} = \langle\phi_{i\sigma}|\frac{1}{\rho_\sigma}\sum_{k=1}^{N_\sigma}|\phi_{k\sigma}|^2 u_{k\sigma}|\phi_{i\sigma}\rangle$, $\bar{u}_\sigma$ is a vector composed of $\bar{u}_{i\sigma}$ values, and M_σ is a matrix given by [29,46]

$$\begin{aligned} M_{ji\sigma} &= \int \frac{|\phi_{j\sigma}(\mathbf{r})|^2|\phi_{i\sigma}(\mathbf{r})|^2}{\rho_\sigma(\mathbf{r})}d\mathbf{r} \\ &= \int \frac{|\phi_{j\sigma}(\mathbf{r})|^2\left[\rho_\sigma(\mathbf{r}) - \sum_{k\neq i}^{N}|\phi_{k\sigma}(\mathbf{r})|^2\right]}{\rho_\sigma(\mathbf{r})}d\mathbf{r} \\ &= 1 - \sum_{k\neq i}^{N} M_{jk\sigma}. \end{aligned} \tag{4}$$

This means that the matrix $I - M_\sigma$ is of the form

$$I - M_\sigma = \begin{pmatrix} 1 - M_{11} & -M_{12} & \cdots & -M_{1N} = -1 + \sum_{i\neq N} M_{1i} \\ -M_{21} & 1 - M_{22} & \cdots & -M_{2N} = -1 + \sum_{i\neq N} M_{2i} \\ \vdots & & \ddots & \\ -M_{N1} & \cdots & & 1 - M_{NN} = \sum_{i\neq N} M_{Ni} \end{pmatrix}. \tag{5}$$

Clearly, the sum of the elements in each row is zero, making the $I-M_\sigma$ matrix singular, such that any constant vector is a null vector of this matrix. As mentioned above, the free constant is usually chosen as $\Delta_{H\sigma} = 0$ to allow for a "natural" asymptotic decay of the KS potential. The HOMO is then removed from the above set of equations, resulting in an $I-M_\sigma$ matrix of size $(N-1)\times(N-1)$ which is no longer singular. However, as the interatomic distance is increased, the orbital overlap between the two atoms decreases in an asymptotically exponential manner and therefore all terms $M_{ij,\sigma}$ where i, j correspond to orbitals on different atoms decay exponentially. Accordingly, if one orders the orbitals by atom, then the $I-M_\sigma$ matrix exponentially approaches a block diagonal form, with each block approaching singularity *individually*. This means that in this limit we have two free constants to choose per each spin channel—one for each atom. Effectively, then, the two atoms have decoupled.

The practical manifestation of the above observation is that with increasing interatomic distance the interatomic orbital overlap becomes numerically negligible and the $(N-1)\times(N-1)$ $I-M_\sigma$ matrix becomes increasingly ill-conditioned. For example, for LiF the determinant of $I-M_\alpha$ used to construct the potential as in Fig. 2 (bottom) decreases by almost three orders of magnitudes as R increases from 8 to 18 a.u. As a consequence, if for $R=18$ a.u. one adjusts the plateau value manually, by additionally fixing the value of $\Delta_{H-1,\alpha}$ as shown in Fig. 5, and recalculates the corresponding total energy, the total energy changes by only $\sim 10^{-5}$ Ry, which is at least two orders of magnitude below the overall accuracy of our calculations, and the density changes by less than 10^{-6} a.u. This manual adjustment is tantamount to an independent choice of the shift for the highest-occupied F orbital. Figure 5 confirms that such a constant shift of the "F domain" with respect to the "Li domain" is indeed the only meaningful difference between the different xKLI potentials obtained from this manual shift. It is also interesting to note that

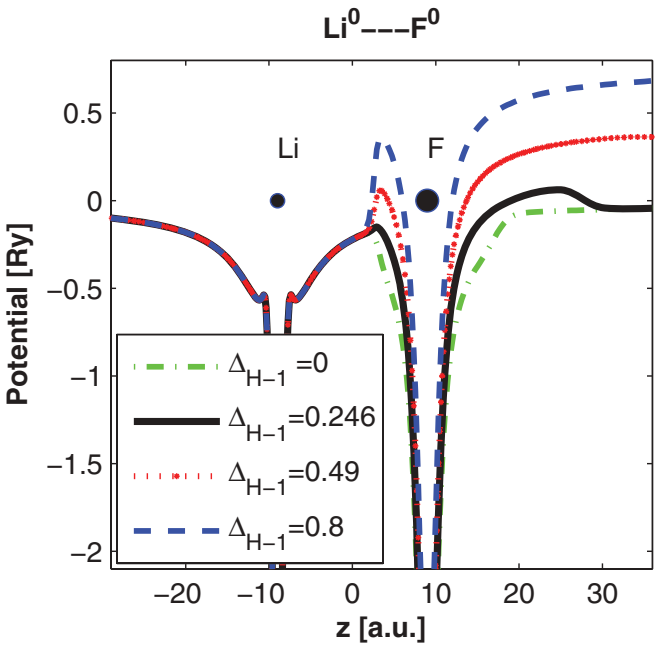

FIG. 5. (Color online) xKLI potentials of $Li^0 \cdots F^0$ with $R = 18$ a.u. in the α-spin channel, corresponding to four different values of $\Delta_{H-1,\alpha}$ (in Ry): 0 (dash-dotted green), 0.246 (thick solid black), 0.49 (dotted red), and 0.8 (dashed blue). The shift given by $\Delta_{H-1,\alpha} = 0.246$ is the one obtained directly from the calculation. All others were manually set.

the larger the relative shift is, the further the plateau extends before reverting back to the asymptotic $-2/r$ curve, i.e., the further out the s_2 step is pushed.

The fact that, within numerical accuracy, several manifestly different potentials effectively share the same ground-state density and total energy may seem to violate the Hohenberg-Kohn theorem [51]. We note that nonuniqueness of the KS map has previously been discussed for spin-polarized DFT [52–54] and explained physically by the need to fix two constants (one for each spin channel) where only one reference energy exists. In our case, however, once the atoms numerically decouple, we effectively deal with two separated subsystems and there are effectively two constants to choose per *each* spin channel. This does not, however, contradict the Hohenberg-Kohn theorem because there now exists a finite region where the density is numerically nonexistent (in the case of Fig. 5 the density is smaller than 10^{-6} along an interatomic segment larger than 1.5 a.u.). For the Hohenberg-Kohn theorem to hold, the ground-state density should not vanish except on a set of zero measure, a condition that is still obeyed analytically, but not numerically. Hence, a unique mapping between the density and the potential no longer exists, unless the numerical accuracy is increased. This also means that, as pointed out previously for the regular spin-polarized case [53], attempts to construct accurate KS potentials out of accurate densities for highly stretched molecules should be performed with great numerical care.

4. Eigenvalue shifts

The eigenvalues obtained from xKLI calculations of Li, F, and $Li^0 \cdots F^0$ (with $R = 18$ a.u.) are listed in Table I. We conclude that the step structure of the xKLI potential is accompanied by a systematic shift in the eigenvalues, as follows. For the α-spin channel, the Li-related eigenvalues of $Li^0 \cdots F^0$ are unchanged, as compared to the majority eigenvalues of Li, whereas the F-related eigenvalues in the same spin channel are shifted by a constant ($\Delta_{H-1,\alpha} = 0.246$ Ry), as compared to the minority eigenvalues of F. A complementary picture is obtained for the β-spin channel—the F-related eigenvalues are unchanged, as compared to the majority eigenvalues of F, but the Li-related eigenvalues are shifted by a constant ($\Delta_{H-4,\beta} = 0.15$ Ry), as compared to the minority eigenvalues of Li. For each spin channel, the atom for which the eigenvalues shift is the same one for which the plateau is observed (see Fig. 2). The only seeming discrepancy is that the F-related eigenvalues of $Li^0 \cdots F^0$ in the α spin are shifted by $\Delta_{H-1,\alpha}$ whereas the potential for the same spin channel is shifted by $\Delta_{H-2,\alpha}$. This is again a consequence of the potential at the bottom part of Fig. 2 having been plotted along the interatomic axis. As discussed above (see Fig. 3), while HOMO-2 dominates the interatomic axis, HOMO-1 is the orbital slowest to decay in almost all directions, and therefore it controls the shift of the eigenvalues.

An important consequence of the above argument is that the relative alignment between the F- and the Li-related eigenvalues in the spin-α channel of $Li^0 \cdots F^0$ is determined solely by the value of $\Delta_{H-1,\alpha}$. Unfortunately, in our xKLI calculations this shift is not large enough, because it places the F-related LUMO below the Li-related HOMO. This explains why the Aufbau principle had to be violated in order to obtain the correct neutral configuration. Had the Aufbau principle been satisfied, the F-related LUMO would have been occupied and the Li-related HOMO would have been unoccupied. Alas, this would mean that the ionic configuration would have been obtained.

Note that there are two different types of Aufbau violations involved. The first one occurs within the Li atom (either as an independent entity or as part of the stretched $Li^0 \cdots F^0$ dimer with $R = 18$ a.u.). The lowest unoccupied minority-spin Li orbital is at -0.605 Ry or -0.454 Ry for the atom or dimer, respectively (in agreement with a shift value of $\Delta_{H-4,\beta} = 0.15$ Ry), i.e., lower in energy than the highest occupied majority-spin orbital (see Table I). This is known as obeying the Aufbau principle only in the broad sense [55]. For the Li atom, this behavior persists even with the exact exchange-correlation functional [56] and is ascribed to the above-discussed nonuniqueness of the KS map for spin-polarized DFT [52–54].

The second violation occurs within the α-spin channel, where the F-related orbital, with an energy of -1.09 Ry, is unoccupied despite being lower in energy than the Li-related HOMO. This violation is more serious as it appears within a given spin channel and thus is outside the formal KS map even in the broad sense. Furthermore, this problem persists even for interatomic distances small enough to avoid the atom decoupling problem discussed above, i.e., it is inherent rather than numerical. Recently, Giesbertz and Baerends [57] have shown that generally the Aufbau principle should hold within each spin channel, if fractional occupations are allowed in the optimization. However, this is rarely done in practice (see

Ref. [58] for a more detailed discussion) and was not attempted here. Whether this violation would persist in the presence of correlation and/or with a full OEP solution remains unknown at present.

IV. CONCLUSIONS

In conclusion, we have examined the role of KS EXX in curing the problem of fractional molecular dissociation. This was achieved by performing EXX calculations for the illustrative case of the LiF molecule. We showed that by choosing the lowest-energy electronic configuration for each interatomic distance, a qualitatively correct binding energy curve, reflecting integer dissociation, was obtained. We demonstrated that this correct result is enforced by the local KS exchange potential via a plateau-like structure, accompanied by two steps, as first suggested for the exact exchange-correlation functional by Perdew [4].

Specifically, we numerically confirmed that the exact-exchange potential of a diatomic molecule is not given by the trivial sum of the corresponding atomic potentials, even when the interatomic distance is arbitrarily large. Instead, one of the atomic potentials is shifted by a constant while the other one is not, depending on where the HOMO is localized, thereby enforcing the integer configuration by preventing spurious charge transfer. We further showed that this structure is an inherent feature of the KLI approximation to the KS potential associated with an orbital-dependent functional. However, this structure becomes increasingly unstable numerically the larger the interatomic separation is, reflecting the increasing absence of coupling between the atoms. Stretched-configuration calculations are therefore numerically challenging, and we have shown here how they can nevertheless be performed. Finally, we discussed the important relation between the step-structure in the KS potential and the accompanying eigenvalue shifts. Our results demonstrate that the EXX functional yields a lowest-energy configuration that correctly dissociates Li and F to neutral atoms, but it does so by violating the Aufbau principle. This is an explicit example of how limited functionals—in our case the limitation is the severe one of complete absence of correlation—can yield reasonable physical results via peculiar detours.

[1] J. P. Perdew, R. G. Parr, M. Levy, and J. L. Balduz, Phys. Rev. Lett. **49**, 1691 (1982).

[2] C.-O. Almbladh and U. von Barth, in *Density Functional Methods in Physics*, edited by R. M. Dreizler and J. da Providencia (Plenum, New York, 1985), Vol. 123 of *NATO ASI Series B: Physics*, pp. 209–231.

[3] J. P. Perdew, in *Density Functional Methods in Physics*, edited by R. M. Dreizler and J. da Providencia (Plenum, New York, 1985), Vol. 123 of *NATO ASI Series B: Physics*, pp. 265–308.

[4] J. P. Perdew, Adv. Quantum Chem. **21**, 113 (1990).

[5] O. V. Gritsenko and E. J. Baerends, Phys. Rev. A **54**, 1957 (1996).

[6] E. J. Baerends and O. V. Gritsenko, J. Phys. Chem. A **101**, 5383 (1997).

[7] M. M. Ossowski, L. L. Boyer, M. J. Mehl, and M. R. Pederson, Phys. Rev. B **68**, 245107 (2003).

[8] A. D. Dutoi and M. Head-Gordon, Chem. Phys. Lett. **422**, 230 (2006).

[9] O. Gritsenko and E. J. Baerends, Int. J. Quantum Chem. **106**, 3167 (2006).

[10] A. Ruzsinszky, J. P. Perdew, G. I. Csonka, O. A. Vydrov, and G. E. Scuseria, J. Chem. Phys. **125**, 194112 (2006).

[11] P. Mori-Sánchez, A. J. Cohen, and W. Yang, J. Chem. Phys. **125**, 201102 (2006).

[12] O. A. Vydrov and G. E. Scuseria, J. Chem. Phys. **125**, 234109 (2006).

[13] O. A. Vydrov, G. E. Scuseria, and J. P. Perdew, J. Chem. Phys. **126**, 154109 (2007).

[14] J. P. Perdew, A. Ruzsinszky, G. I. Csonka, O. A. Vydrov, G. E. Scuseria, V. N. Staroverov, and J. Tao, Phys. Rev. A **76**, 040501(R) (2007).

[15] A. J. Cohen, P. Mori-Sánchez, and W. Yang, Science **321**, 792 (2008).

[16] E. Sagvolden and J. P. Perdew, Phys. Rev. A **77**, 012517 (2008).

[17] A. Karolewski, R. Armiento, and S. Kümmel, J. Chem. Theory Comput. **5**, 712 (2009).

[18] D. G. Tempel, T. J. Martínez, and N. T. Maitra, J. Chem. Theory Comput. **5**, 770 (2009).

[19] J. P. Perdew, A. Ruzsinszky, L. A. Constantin, J. Sun, and G. I. Csonka, J. Chem. Theory Comput. **5**, 902 (2009).

[20] N. Helbig, I. V. Tokatly, and A. Rubio, J. Chem. Phys. **131**, 224105 (2009).

[21] R. Baer, E. Livshits, and U. Salzner, Annu. Rev. Phys. Chem. **61**, 85 (2010).

[22] J. I. Fuks, A. Rubio, and N. T. Maitra, Phys. Rev. A **83**, 042501 (2011).

[23] S. Kümmel and L. Kronik, Rev. Mod. Phys. **80**, 3 (2008).

[24] J. P. Perdew and A. Zunger, Phys. Rev. B **23**, 5048 (1981).

[25] W. Kohn and L. J. Sham, Phys. Rev. **140**, A1133 (1965).

[26] T. Körzdörfer, M. Mundt, and S. Kümmel, J. Chem. Phys. **129**, 014110 (2008).

[27] R. T. Sharp and G. K. Horton, Phys. Rev. **90**, 317 (1953).

[28] J. D. Talman and W. F. Shadwick, Phys. Rev. A **14**, 36 (1976).

[29] T. Grabo, T. Kreibich, and E. K. U. Gross, Mol. Eng. **7**, 27 (1997).

[30] E. Engel, *A Primer in Density Functional Theory* (Springer, Berlin, 2003), Chap. 2, pp. 56–122.

[31] A. Görling, J. Chem. Phys. **123**, 062203 (2005).

[32] Evidence for the special case of LiH, where both cation and anion are effectively one-electron systems due to the use of pseudopotentials, have been recently given in Ref. [22].

[33] M. Mundt and S. Kümmel, Phys. Rev. Lett. **95**, 203004 (2005).

[34] I. Dreissigacker and M. Lein, Chem. Phys. (to appear), doi:10.1016/j.chemphys.2011.02.009

[35] A. Makmal, S. Kümmel, and L. Kronik, J. Chem. Theory Comput. **5**, 1731 (2009).

[36] J. B. Krieger, Y. Li, and G. J. Iafrate, Phys. Rev. A **45**, 101 (1992).

[37] R. S. Mulliken, J. Chem. Phys. **23**, 1833 (1955).
[38] R. F. W. Bader and P. M. Beddall, J. Chem. Phys. **56**, 3320 (1972).
[39] F. L. Hirshfeld, Theoret. Chim. Acta (Berl.) **44**, 129 (1977).
[40] C. A. Coulson and I. Fischer, Philos. Mag. **40**, 386 (1949).
[41] M. Levy, J. P. Perdew, and V. Sahni, Phys. Rev. A **30**, 2745 (1984).
[42] C.-O. Almbladh and U. von Barth, Phys. Rev. B **31**, 3231 (1985).
[43] J. B. Krieger, Y. Li, and G. J. Iafrate, in *Density Functional Theory* (Plenum, New York, 1995), p. 191.
[44] F. Della Sala and A. Görling, Phys. Rev. Lett. **89**, 033003 (2002).
[45] T. Kreibich, S. Kurth, T. Grabo, and E. K. U. Gross, Adv. Quantum Chem. **33**, 31 (1998).
[46] F. Della Sala and A. Görling, J. Chem. Phys. **115**, 5718 (2001).
[47] F. Della Sala and A. Görling, J. Chem. Phys. **116**, 5374 (2002).
[48] S. Kümmel and J. P. Perdew, Phys. Rev. B **68**, 035103 (2003).
[49] R. van Leeuwen, O. Gritsenko, and E. J. Baerends, Z. Phys. D **33**, 229 (1995).
[50] M. Cinal, J. Chem. Phys. **132**, 014101 (2010).
[51] P. Hohenberg and W. Kohn, Phys. Rev. **136**, B864 (1964).
[52] H. Eschrig and W. E. Pickett, Solid State Commun. **118**, 123 (2001).
[53] K. Capelle and G. Vignale, Phys. Rev. Lett. **86**, 5546 (2001).
[54] P. W. Ayers and W. Yang, J. Chem. Phys. **124**, 224108 (2006).
[55] E. Kraisler, G. Makov, and I. Kelson, Phys. Rev. A **82**, 042516 (2010).
[56] O. V. Gritsenko and E. J. Baerends, J. Chem. Phys. **120**, 8364 (2004).
[57] K. J. H. Giesbertz and E. J. Baerends, J. Chem. Phys. **132**, 194108 (2010).
[58] P. R. T. Schipper, O. V. Gritsenko, and E. J. Baerends, Theor. Chem. Acc. **99**, 329 (1998).